Title

Changes in river water temperature between 1980 and 2012 in Yongan watershed, eastern China: Magnitude, drivers and models

Permalink

https://escholarship.org/uc/item/8cg42512

Authors

Chen, Dingjiang
Hu, Minpeng
Guo, Yi
et al.

Publication Date

DOI

Peer reviewed

Changes in river water temperature between 1980 and 2012 in Yongan watershed, eastern China: Magnitude, drivers and models

Dingjiang Chen [a,b,*], Minpeng Hu [a,b], Yi Guo [a,c], Randy A. Dahlgren [d]

[a] College of Environmental & Resource Sciences, Zhejiang University, Hangzhou 310058, China
[b] Ministry of Education Key Laboratory of Environment Remediation and Ecological Health, Zhejiang University, Hangzhou 310058, China
[c] Zhejiang Provincial Key Laboratory of Subtropical Soil and Plant Nutrition, Zhejiang University, Hangzhou 310058, China
[d] Department of Land, Air, and Water Resources, University of California, Davis, CA 95616, USA

ARTICLE INFO

SUMMARY

Climate warming is expected to have major impacts on river water quality, water column/hyporheic zone biogeochemistry and aquatic ecosystems. A quantitative understanding of spatio-temporal air (T_a) and water (T_w) temperature dynamics is required to guide river management and to facilitate adaptations to climate change. This study determined the magnitude, drivers and models for increasing T_w in three river segments of the Yongan watershed in eastern China. Over the 1980–2012 period, T_w in the watershed increased by 0.029–0.046 °C yr^{-1} due to a ~0.050 °C yr^{-1} increase of T_a and changes in local human activities (e.g., increasing developed land and population density and decreasing forest area). A standardized multiple regression model was developed for predicting annual T_w (R^2 = 0.88–0.91) and identifying/partitioning the impact of the principal drivers on increasing T_w:T_a (76 ± 1%), local human activities (14 ± 2%), and water discharge (10 ± 1%). After normalizing water discharge, climate warming and local human activities were estimated to contribute 81–95% and 5–19% of the observed rising T_w, respectively. Models forecast a 0.32–1.76 °C increase in T_w by 2050 compared with the 2000–2012 baseline condition based on four future scenarios. Heterogeneity of warming rates existed across seasons and river segments, with the lower flow river and dry season demonstrating a more pronounced response to climate warming and human activities. Rising T_w due to changes in climate, local human activities and hydrology has a considerable potential to aggravate river water quality degradation and coastal water eutrophication in summer. Thus it should be carefully considered in developing watershed management strategies in response to climate change.

© 2015 Elsevier B.V. All rights reserved.

1. Introduction

Water temperature is an important river physical property with a crucial impact on aquatic ecosystem health, as most river biogeochemical processes are functions of temperature (Webb and Nobilis, 2007; Webb et al., 2008; Kaushal et al., 2010; evan Vliet et al., 2012; Xin and Kinouchi, 2013; Luce et al., 2014; Rice and Jastram, 2015). Higher water temperature can impair the habitat of a wide range of aquatic organisms from invertebrates to salmonids (Langan et al., 2001; Caissie, 2006; Isaak et al., 2012; Markovic et al., 2013; Null et al., 2013a,b), as well as degrade water quality such as decreased oxygen-holding capacity, increased oxygen consumption, and enhanced formation of potentially toxic NH_3 (Webb

and Nobilis, 2007; Pekárová et al., 2011; El-Jabi et al., 2014). Furthermore, increasing riverine heat flux has a great potential to aggravate eutrophication (including harmful algal blooms) and hypoxia in downstream lakes, estuaries and coastal waters (Liu et al., 2005; Ozaki et al., 2008; Ye et al., 2011; Rice and Jastram, 2015), as well as to impair their biological communities (Seekell and Pace, 2011).

Various studies have shown that rising water temperature is strongly related to climate warming across a range of river types (e.g., watershed size) and time scales (e.g., daily, weekly, monthly, and annual), because air temperature is a major component in calculating net heat fluxes at the air–water interface (Webb et al., 2003, 2008; Caissie, 2006). For example, Seekell and Pace (2011) indicated that a 0.945 °C increase of water temperature in the Hudson River during the period 1946–2008 was primarily related to air temperature increasing. Depending on the river type and time scale, the air–water temperature dynamics can be effectively

expressed by a linear or logistic function (Mohseni and Stefan, 1999; Webb et al., 2003; Pekárová et al., 2011; van Vliet et al., 2012; Gu et al., 2014). For example, the slopes of the regression lines between water and air temperature generally increase with increasing time scales (daily, weekly, monthly and annually), while the slope decreases from small upstream to large downstream river reaches (Webb et al., 2003; Caissie, 2006). For some groundwater-dominated rivers, due to the influence of groundwater inputs at low air temperature and evaporative cooling at high air temperature, weekly or daily air–water temperature relationships often departure from a linear relationship and are better expressed by a logistic regression (Caissie, 2006; Webb et al., 2003, 2008).

Although the relationship between air and water temperature is generally strong, the strength of such a relationship varies regionally and temporally, and can be highly site specific due to additional influences from local hydrology and human activities, such as changes in land-use and population density (Arismendi et al., 2012; Orr et al., 2015; DeWeber and Wagner, 2014). It is commonly observed that water temperature is inversely related to river discharge, reflecting a reduced thermal buffering capacity due to decreasing flow volumes, increasing travel time, and diminished dilution capacity for inputs of thermal effluents (Gu and Li, 2002; Webb et al., 2003; Moatar and Gailhard, 2006; Albek and Albek, 2009). A global assessment indicated that a decrease in river discharge by 20% and 40% would exacerbate water temperature increases by 0.3 °C and 0.8 °C on average, respectively, in addition to a 2–6 °C increase due to rising air temperature (van Vliet et al., 2011). Furthermore, rivers with low groundwater inputs are generally more sensitive to changes in air temperature compared with groundwater-dominated rivers (Caissie, 2006).

Regarding land-use change, many studies suggest that decreasing forest area (or decreasing vegetation shading (Moore et al., 2005; Ozaki et al., 2008; Pekárová et al., 2011; Simmons et al., 2014) and increasing urban area (or increasing human density and increasing thermal effluent) within a catchment can significantly increase river water temperature in addition to climate warming (Langan et al., 2001; Caissie, 2006; Albek and Albek, 2009; Xin and Kinouchi, 2013; Gu et al., 2014; Lepori et al., 2014; Orr et al., 2015). For example, the observed water temperature increases of 0.11–0.21 °C yr^{-1} in winter and spring for some stream segments in central Tokyo and its suburbs between 1978 and 1998 were ascribed to increases in anthropogenic heat input from urban wastewater (Kinouchi, 2007). Other human activities, such as river diversion, channelization and impoundments, can also alter the thermal dynamics of downstream reaches (Liu et al., 2005; Žganec, 2012; Null et al., 2013a,b).

While it has been recognized that increasing river water temperature is a complex function of the interaction of changes in climate, hydrology, and human activities, there is a distinct paucity of studies that address their integrated influence on spatio-temporal river water temperature dynamics due to a lack of long-term data sets (Caissie, 2006). Importantly, little quantitative knowledge is available concerning what contribution of the river warming rate is attributable to climate warming versus local human activities. Such quantitative information is critical for developing effective watershed management plans and water quality standards to protect aquatic species (Moatar and Gailhard, 2006; Caissie, 2006; Kaushal et al., 2010).

Although long-term trend analyses of river water temperature have been widely examined in American and European watersheds, little knowledge is available for rivers in China. Examining long-term river water temperature trends is especially important for watersheds in eastern China that have experienced rapid economic development, human population expansion, and urbanization, as well as significant climate change since the 1980s

(Huang et al., 2014; Chen et al., 2014). For coastal waters along the East China Sea, serious algal blooms and persistent hypoxia have been widely reported in recent decades (Li et al., 2007; Gao and Zhang, 2010). From the perspective of future global warming and increased human activities, higher temperature of water from upstream rivers has the potential to greatly aggravate eutrophication (including harmful algal blooms) and hypoxia of downstream coastal waters. These effects are exacerbated by increasing inputs of oxygen-demanding substances and excessive nutrients in many rivers in eastern China (Huang et al., 2014). Accordingly, it is urgent to gain a comprehensive and quantitative understanding of long-term water temperature trends in response to changes in air temperature, hydrology, and human activities for rivers in eastern China.

This study provides the first historical analysis of river water temperature changes in response to changes in climate, hydrology, and human activities for a rapidly developing watershed (i.e., Yongan watershed) in eastern China over the 1980–2012 period. Human activities in this study are defined as increasing developed land, decreasing forest land, and increasing population. Three river segments located in headwater, mid-watershed, and lowland portions of the Yongan watershed were selected for analysis to provide a range in levels of human disturbance and water discharge conditions. This study advances our understanding of river water temperature dynamics by (i) examining the long-term warming rates of annual and monthly river water temperature as well as their spatial heterogeneities, (ii) addressing the drivers of the observed rising river water temperature, (iii) developing a standardized multiple regression model for predicting river water temperature, (iv) identifying individual contributions of climate warming and human activities to rising water temperature, and (v) forecasting trends in river water temperature based on scenarios for future (2013–2050) changes in climate and human activities expected for this watershed. Besides being the first analysis of river water temperature dynamics in China, novel aspects of this study include demonstrating the integrated influence of air temperature, hydrology, and human activities on the spatio-temporal river water temperature dynamics and providing a simple methodology for quantifying the contributions of the identified drivers to variations of river water temperature. The results of this study improve our quantitative understanding of long-term annual, seasonal, and spatial air and water temperature dynamics for improving watershed management and facilitating adaptation to these climate change effects.

2. Materials and methods

2.1. Study watershed

The Yongan watershed (120.2295°–121.0146°E and 28.4695°–29.0395°N; elevation ~15–1000 m) is located in the rapidly developing Taizhou region of Zhejiang Province, China (Fig. 1). The Yongan River is the third largest river of Zhejiang Province and flows into Taizhou Estuary and the East China Sea, a coastal area that commonly experiences hypoxia (Li et al., 2007; Gao and Zhang, 2010). The river drains 2474 km^2 and has an average water depth of 5.42 m and discharge of 72.9 m^3 s^{-1} at the downstream BZA sampling site (Fig. 1). The climate is subtropical monsoon having an average annual temperature of 17.2 °C (16.3–18.6 °C) and average annual precipitation of 1395 mm (1064–1813 mm). Rainfall mainly occurs in May–September (67% of total annual precipitation) with a typhoon season in July–September, while winter (December, January and February) is a major dry season receiving only 15% of the annual precipitation. There are no major dams/reservoirs or water withdrawals/transfers in the watershed.
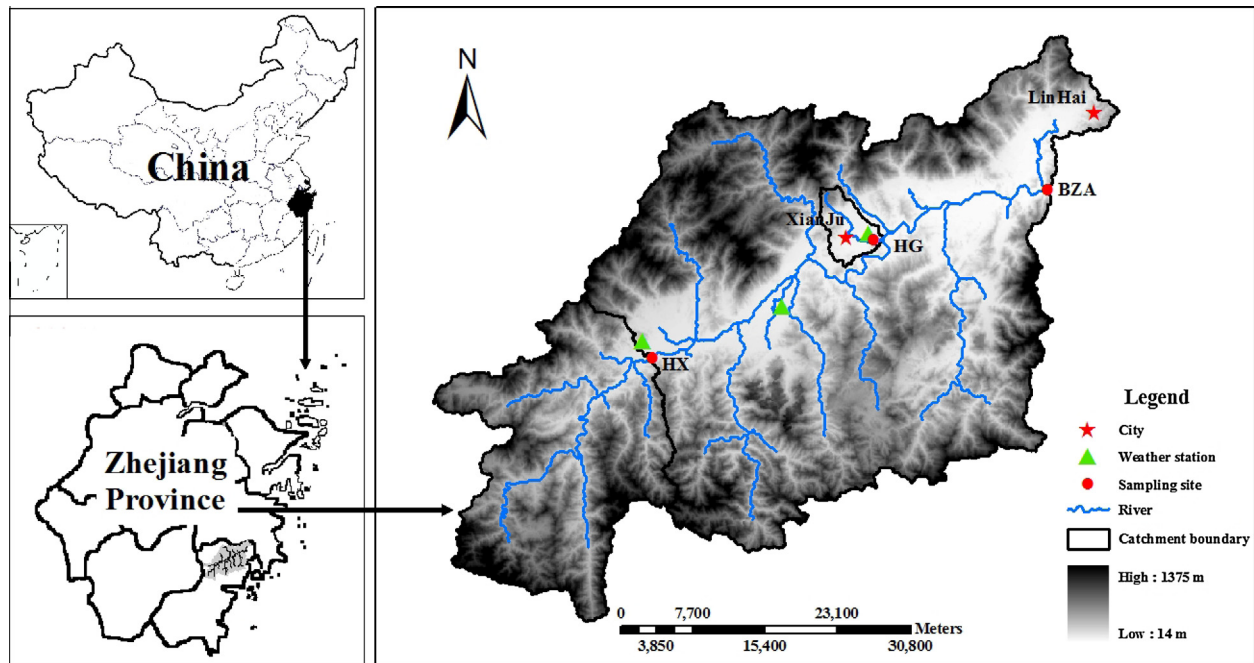
Fig. 1. The location the Yongan River watershed in China and Zhejiang Province and the three water temperature monitoring sites and three weather stations.

Three river segments consisting of headwater (upstream), mid-watershed and lowland (downstream) components (i.e., HX, HG, and BZA, Fig. 1) were selected to provide a range in levels of human development and water discharge conditions (Table 1). Among them, catchment HG had the highest percentage of developed land, as well as the highest human and domestic animal densities. Over the 33-year study period, human population and developed land area within the three catchments increased by 27–32% and 60–80%, respectively, while forest land decreased by 6–12% (Table 1).

2.2. Data collection

Monthly mean river water temperatures at the three hydrologic stations (Fig. 1) during the 1980–2012 period were provided by the local Hydrology Bureau. River water temperature was measured during daytime once to thrice every month using a consistent method throughout the study period. The measurements were consistently made in the middle of the river section in flowing water deeper than 0.3–0.5 m. During measurements, a mercurial thermometer (limit of detection: LOD = 0.1 °C) was installed inside an empty bottle and placed 0.3–0.5 m below the water surface for 5–8 min. Following filling of the bottle and equilibration, the bottle

containing the river water sample was retrieved and the temperature immediately recorded. Data were available for the full 33-year period for sites HX and BZA, and for 26 years at site HG.

Daily river discharge data for the three sampling sites within the Yongan watershed (Fig. 1) over the 1980–2012 period were provided by the local Hydrology Bureau. River discharge was measured once every 2–12 h (more frequently during storm events) using the rotating-element current-meter method. Daily air temperature data for the three weather monitoring stations within the Yongan watershed (Fig. 1) over the 1980–2012 period were obtained from the local Weather Bureau. The upstream, mid-watershed and downstream weather monitoring stations (Fig. 1) were located in rural, rural and suburban regions, respectively. According to the standard methods for weather observations, air temperature was recorded once every 2 h from a mercurial thermometer (limit of detection: LOD = 0.1 °C) installed within a standard thermometer shelter 1.5 m above the ground.

Data concerning land use and human population for the three catchments of the Yongan watershed from 1980 to 2012 were obtained from the annual Statistic Yearbooks of Xianju County and Linhai City. By defining the watershed boundary using a geographical information system (GIS), all twenty towns within Xianju

Table 1
Characteristics of land-use distribution, population, water discharge and runoff coefficient for the three catchments of the Yongan River watershed over the 1980–2012 period.

Catchments	Periods	Land use			Population (capita km^{-2})	Discharge (m^3 s^{-1})	Runoff coefficient[a]
		Agricultural (%)	Developed (%)	Forest (%)			
HX (Area: 547 km^2) (Elevation: 538 m)	1980s	7	1	92	122	16.0	0.65
	1990s	7	1	92	130	17.1	0.65
	2000s	9	2	90	148	15.6	0.60
HG (Area: 35 km^2) (Elevation: 139 m)	1980s	18	7	76	704	1.0	0.72
	1990s	17	7	73	744	1.1	0.73
	2000s	20	10	70	830	1.0	0.67
BZA (Area: 2474 km^2) (Elevation: 438 m)	1980s	11	2	87	248	72.2	0.67
	1990s	11	3	86	266	77.5	0.68
	2000s	13	3	84	288	70.7	0.62

[a] Runoff coefficient denotes the ratio between annual total runoff depth and precipitation.

County (~73% of total watershed area) and one town in Linhai City (~12% of total watershed area) were included within the watershed boundary. The remaining ~15% of the watershed area was dominated by forests (~95%) and fell within Panan County (located in the northwest portion of the watershed) and Jinyun County (located in the southwest portion of the watershed) (Fig. 1). Relevant data over the past 33 years for this remaining area were extrapolated from the nearby towns that have similar forest area percentages (90–96%).

2.3. Statistical analyses

To detect the trends in air temperature, river water temperature and discharge over the 1980–2012 period, a linear regression analysis was adopted to establish the relationship between each of variables and year number over the study period (Kaushal et al., 2010; Chen et al., 2014; Rice and Jastram, 2015). When regression equations were statistically significant ($p < 0.05$), the change in rate or percentage was determined by the regression slope. In this study, all correlation analyses, regression analyses and analysis of variance (ANOVA) were performed using SPSS statistical software (version 16.0, SPSS Inc., USA, 2002).

To address the quantitative response of annual mean river water temperature (T_w, °C) to potential drivers (i.e., changes in air temperature, hydrology, and human activities), this study used a standardized multiple regression model:

$$T_w = a + \sum_{i=1}^{n} b_i x_i \qquad (1)$$

where x_i is the factors (e.g., standardized annual air temperature, water discharge, developed land area percentage, population density, and forest area percentage) influencing river water temperature, and a and b_i are regression parameters. In this study, all individual factors were standardized to the same scale by scaling as a function of the maximum value over the study period for all sites.

To determine the most influential drivers for the model, the potential influencing factors were added stepwise for x_i to calibrate the regression parameters. The optimized set of influencing factors was determined according to the highest model agreement. The agreement between observed and modeled annual mean water temperature was evaluated using correlation (R^2) and Nash–Sutcliffe coefficients (Huang et al., 2014). Regression analysis was applied to calibrate the parameters α and b_i in Eq. (1).

Based on the developed standardized multiple regression models, the contribution (c_i) of individual drivers to temporal or spatio-temporal variation of annual water temperature was estimated by:

$$c_i = \frac{|b_i|}{\sum_{i=1}^{n} |b_i|} \qquad (2)$$

3. Results

3.1. Long-term trend and spatial heterogeneity in annual water temperature

Over the 1980–2012 period, annual mean air temperature at the upstream, mid-watershed and downstream sampling sites was 16.9 ± 0.5 °C, 17.6 ± 0.6 °C, and 17.3 ± 0.6 °C, respectively (Fig. 1). In comparison, annual mean water temperature for river segment HX, HG, and BZA was 17.8 ± 0.4 °C, 19.5 ± 0.6 °C, and 19.4 ± 0.5 °C, respectively (Fig. 2). Each river segment had a significant ($p < 0.01$) overall positive trend in annual river water temperature from 1980 to 2012 with warming rates of 0.029–0.046 °C yr^{-1}. This

equates to an increase in river water temperature of 0.96–1.51 °C during the study period.

These increasing water temperature trends coincide with an increase in air temperature of 0.050–0.051 °C yr^{-1} during the study period (Table 2). Furthermore, the increase of water temperature was also affected by a 60–80% increase in developed land area, a 27–32% increase in population density, and a 6–12% decrease in forest land area (Table 2). Although there were no significant trends in annual mean river discharge (Fig. 2, $p > 0.05$) over the study period, water temperature was inversely correlated ($p < 0.05$) with discharge in each river segment (Table 2).

Among the three river segments, HX having a higher elevation and greater than 90% forest cover (Table 1) had the lowest annual mean water temperature of 17.8 ± 0.4 °C, as well as the lowest warming rate of 0.029 °C yr^{-1} (Fig. 3). River segment HG with a lower elevation and greater than 7% developed land area and a population density of 700 capita km^{-2} had the highest mean water temperature of 19.5 ± 0.6 °C, as well as the highest warming rate of 0.046 °C yr^{-1}. The coefficient of variation (CV) for annual mean water temperature during the study period followed the order: HG (CV = 0.028) > BZA (CV = 0.025) > HX (CV = 0.020), compared to CV values of 0.035 to 0.036 for air temperature. These results imply that the river segment having more human activities has a larger temporal variability in water temperature, and air temperature presented a larger temporal variability than water temperature.

3.2. Long-term trend and spatial heterogeneity in seasonal water temperature

As expected, summer (i.e., June, July, and August) and winter (i.e., December, January, and February) have the highest and lowest water temperatures in each river segment, respectively (Fig. 3). For the majority of months, river segments HX, HG, and BZA showed significant positive trends in monthly mean water temperature from 1980 to 2012 ($p < 0.05$), with warming rates of 0.013–0.054 °C yr^{-1}, 0.027–0.061 °C yr^{-1} and 0.015–0.051 °C yr^{-1}, respectively (Fig. 4). These river warming rates were coincident with warming rates observed in monthly air temperatures ($p < 0.05$, Fig. 4) and displayed negative correlations with river discharge ($p < 0.05$). As a result, the dry winter season had a higher warming rate of 0.045–0.057 °C yr^{-1} for monthly mean water temperature than other seasons in each river segment. There were lag effects between changes in monthly air and water temperatures (Fig. 5a) indicated by significant correlations between monthly mean water temperature and previous month's air temperature, especially for the previous 1–3 months ($R^2 > 0.90$). This result is apparent from the high autocorrelations ($R^2 > 0.50$) observed between monthly mean water temperature and the previous 1–2 month's mean water temperature (Fig. 5b).

Among the three river segments, HG and HX had the highest and lowest seasonal mean temperatures, respectively, while there were no significant differences for HG and BZA during the summer and fall seasons (Fig. 3). Remarkably, the warming rate (0.53–0.61 °C yr^{-1}) of HG during the dry winter season exceeded the warming rate (0.46–0.56 °C yr^{-1}) of the air temperature (Fig. 4). Furthermore, river segment HG and BZA having the smallest and largest catchment areas showed the smallest and largest lag effect with air temperature, respectively (Fig. 5).

3.3. Regression models for modeling annual river water temperature

Considering the influence of air temperature, water discharge, and local human activities (i.e., changes in land use or population density), we developed standardized multiple regression models for annual mean water temperature for each river segment
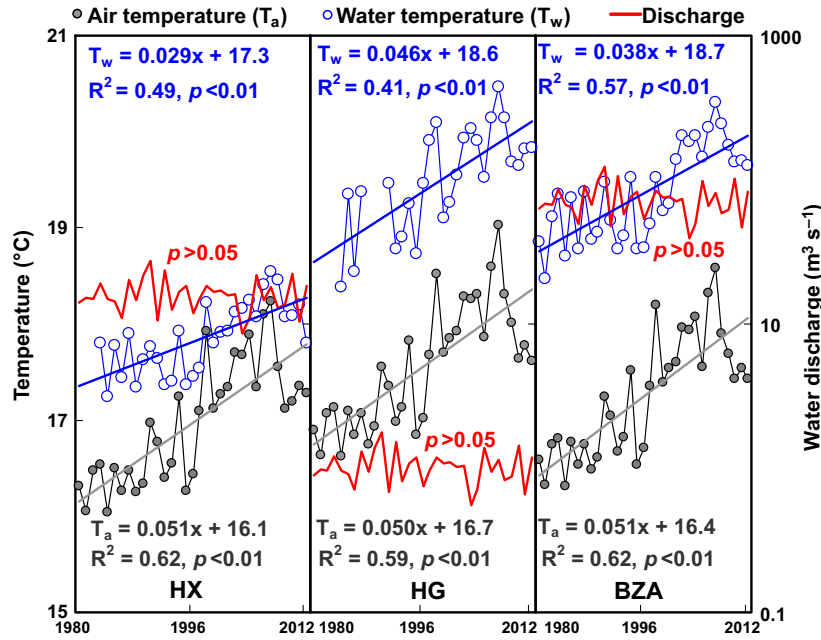
Fig. 2. Historical trends of annual mean river water temperature, air temperature, and water discharge in the three catchments of the Yongan River watershed over the 1980–2012 period.

Table 2
Regression models between annual mean river temperature (T_w, °C) and air temperature (T_a, °C), discharge (Q, m³ s⁻¹), forest area percentage ($F\%$), developed land area percentage ($D\%$), and population density (P, capita km⁻²) for the three river segments of the Yongan River watershed over the 1980–2012 period.

River	Regression equations	R^2	n
HX	$T_w = 0.52T_a + 9.04$	0.81[**]	32
	$T_w = -0.031Q + 18.35$	0.15[*]	32
	$T_w = -14.89F\% + 31.35$	0.46[**]	32
	$T_w = 2.15P + 14.92$	0.56[**]	32
	$T_w = 59.44D\% + 16.95$	0.33[**]	32
HG	$T_w = 0.75T_a + 6.19$	0.76[**]	26
	$T_w = -1.047Q + 20.56$	0.22[**]	26
	$T_w = -7.41F\% + 24.88$	0.32[**]	26
	$T_w = 0.60P + 14.84$	0.47[**]	26
	$T_w = 13.12D\% + 18.45$	0.21[*]	26
BZA	$T_w = 0.70T_a + 7.32$	0.82[**]	33
	$T_w = -0.011Q + 20.12$	0.15[*]	33
	$T_w = -20.95F\% + 37.22$	0.52[**]	33
	$T_w = 1.92P + 14.18$	0.58[**]	33
	$T_w = 51.55D\% + 17.89$	0.39[**]	33

[*] $p < 0.05$.
[**] $p < 0.01$.

Fig. 3. Difference in annual and seasonal water temperature among the three river segments of the Yongan River watershed over the 1980–2012 period. Lower case letters denote significant differences ($p < 0.05$).

In terms of spatio-temporal dynamics, the three models developed for the combined river segments, which simultaneously considered air temperature, water discharge, and developed land area percentage/forest area percentage/population density as the independent variables, accounted for 88–91% of the variation in annual water temperature for the three river segments (Table 3). Average prediction errors for the combined river models were less than 10% and Nash–Sutcliffe coefficients were greater than 0.87. Further incorporation of two land-use factors (i.e., developed land area percentage and forest area percentage) did not improve the predictive capabilities of the models ($R^2 = 0.85$–0.88; Nash–Sutcliffe coefficient = 0.84–0.88) due to the significant autocorrelation among these three inter-related human activity factors ($R^2 = 0.64$–0.76).

3.4. Contribution of influencing factors (drivers) to annual river water temperature

Based on the standardized multiple regression models (Table 3), we apportioned the contribution of individual influencing factors

independently as well as the three river segments combined using Eq. (1). Compared to the individual variables alone (Table 2), combining air temperature and either land use or population density or water discharge in the regression models explained temporal and spatio-temporal variations of annual river water temperature more accurately (Table 3). As expected, the predictive capability was further improved by combining air temperature, water discharge, and land use or population density. The three models developed for individual river segments, which simultaneously considered air temperature, water discharge, and developed land area percentage/forest area percentage/population density as the independent variables, accounted for 94–97% of the temporal variation in annual water temperature over the study period (Table 3). Average prediction errors for these models were less than 6% and Nash–Sutcliffe coefficients were greater than 0.94.
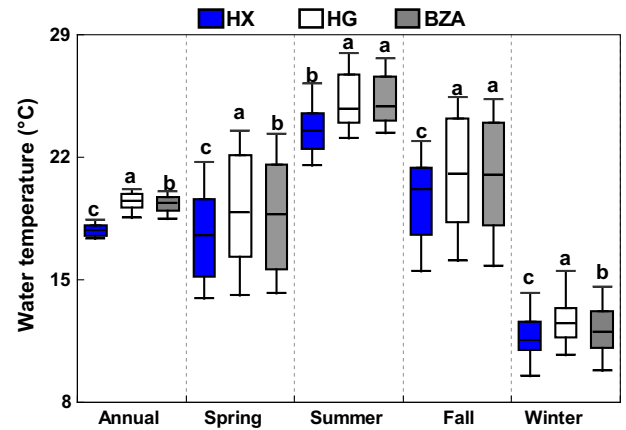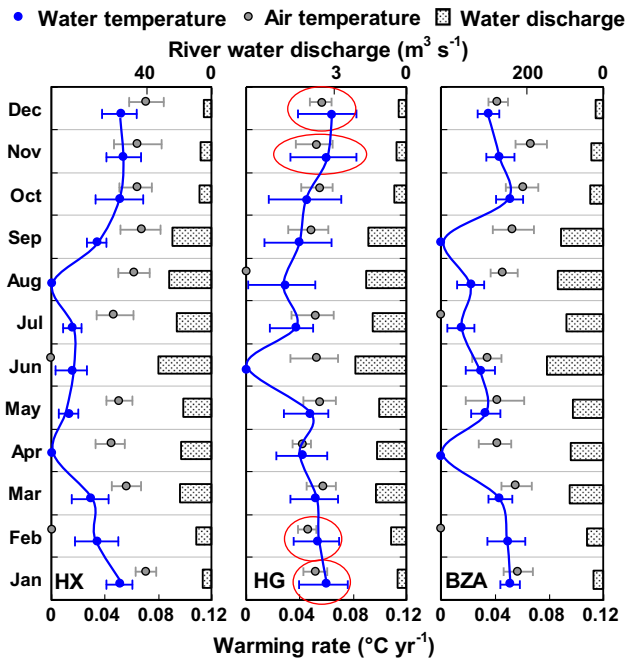
Fig. 4. Historical trends of monthly mean river water temperature, air temperature, and water discharge in the three river segments of the Yongan River watershed over the 1980–2012 period. Error bars denote the 95% confidence interval of the warming rate.

(i.e., drivers) to observed variations of annual river water temperature using Eq. (2). The three standardized regression models developed for individual river segments consistently estimated that annual air temperature accounted for 90 ± 1%, 77 ± 2%, and 83 ± 2% of the temporal variation in water temperature for river segment HX, HG and BZA, respectively (Fig. 6a). Water discharge contributed 5–6% of the temporal variation in annual water temperature for each river segment. In addition, changes in land use or population density contributed to 5–18% of the annual variation in river temperature with the highest contribution occurring in HG. After normalizing for the effects of water discharge on water temperature (Table 2), the climate warming and local human activities were estimated to account for 81–95% and 5–19% of rising water temperature, respectively.

In terms of spatio-temporal dynamics, the three models developed for the combined river segments consistently estimated that annual air temperature, water discharge, and local human activities contributed 76 ± 1%, 10 ± 1% and 14 ± 2%, respectively, of the variations in river temperature for the three river segments

(Fig. 6a). After normalizing for river discharge, the climate warming and local human activities contributed 84% and 16%, respectively, to the rising river water temperature on average for this watershed. These results were comparable to the results estimated separately for each independent river segment (Fig. 6a).

3.5. Predicting future river water temperature

To forecast river water temperature for 2050 using the developed standardized regression models for each river segment (Table 3), average air temperature and water discharge in 2000–2012 and land use or population density in 2012 were consider as baseline conditions. We forecasted future annual river temperatures based on four scenarios that bracket the range of expected conditions for the Yongan watershed.

The "climate change I" scenario projects a 0.76 °C increase of air temperature by 2050 based on the warming rate (0.02 °C yr^{-1}) predicted by the IPCC (2013) with no changes in land use, population and water discharge. This scenario predicted a 0.32–0.45 °C increase of river water temperature by 2050 relative to baseline conditions (Fig. 6b).

The "climate change II" scenario assumes a 1.94 °C increase of air temperature by 2050 based on the warming rate observed over the 1980–2012 period (Fig. 2) with no changes in land use, population and water discharge. This scenario predicted a 0.91–1.41 °C increase of river water temperature by 2050 relative to baseline conditions (Fig. 6b).

The "climate change III" scenario projects a 1.94 °C increase of air temperature and 7% increase in water discharge by 2050 (~0.2% increase per year, Huang et al., 2014) with no change in land use and population. This scenario predicted a 0.85–1.30 °C increase of river water temperature by 2050 relative to baseline conditions (Table 3).

Under the "developing" scenario, river water temperature is expected to increase by 1.12–1.76 °C in 2050 due to a 1.94 °C increase of air temperature combined with a 7–14% decrease in forest area or 69–92% increase in developed land area or 31–37% increase in population density compared to baseline conditions.

For the four scenarios, predicted water temperatures for river segments HG and HX showed the highest and lowest response to changes in future air temperature and land use or population, respectively (Fig. 6b).

4. Discussion

For the Yongan River watershed, the observed warming rates in river water temperature (0.029–0.046 °C yr^{-1}, Fig. 2) over the 1980–2012 period are comparable with long-term observations
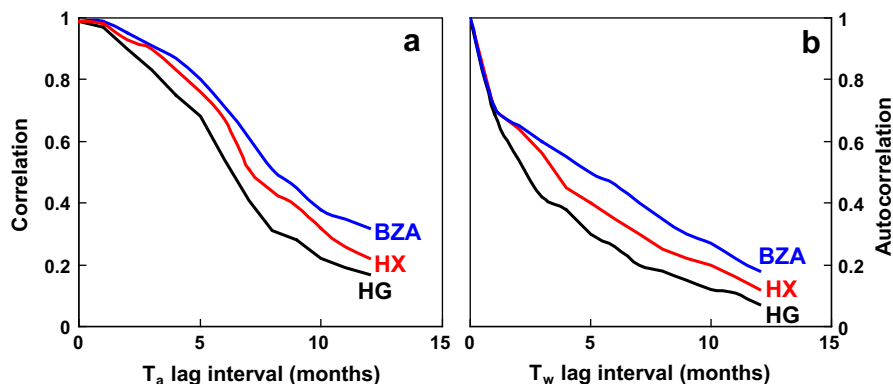
Fig. 5. Linear correlation between monthly mean water temperature (T_w) and air temperature (T_a) (a) and linear autocorrelation for T_w (b) with lag-interval (months) in the three river segments of the Yongan River watershed over the 1980–2012 period.
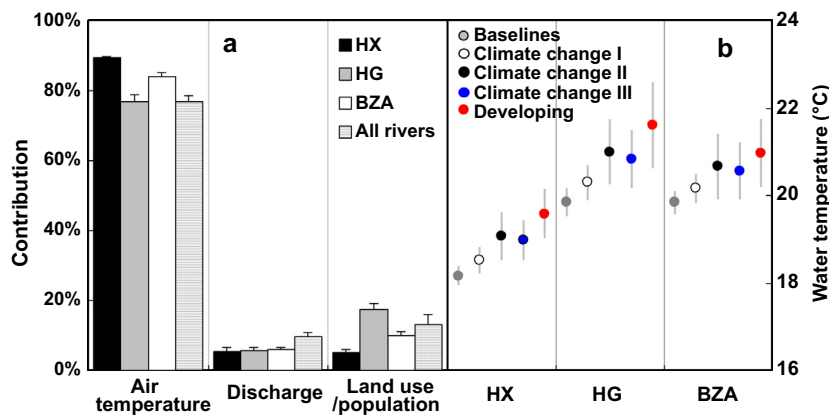
Table 3
Standardized multiple regression models for annual mean water temperature (T_w, °C) of each river segment and all three river segments of the Yongan River watershed over the 1980–2012 period.

River	Model formats	R^2	Nash–Sutcliffe coefficient	Relative error (%)	n
HX	$T_w = 9.46 \times t_a - 0.38 \times q + 9.00$	0.88	0.87	±12	32
	$T_w = 8.27 \times t_a + 0.65 \times p + 9.56$	0.90	0.91	±9	32
	$T_w = 8.56 \times t_a + 0.43 \times d\% + 9.60$	0.92	0.91	±8	32
	$T_w = 8.06 \times t_a - 0.47 \times f\% + 9.71$	0.90	0.89	±10	32
	$\mathbf{T_w = 7.57 \times t_a - 0.47 \times q - 0.47 \times f\% + 10.14}$	**0.95**	**0.94**	**±6**	**32**
	$\mathbf{T_w = 7.99 \times t_a - 0.38 \times q + 0.35 \times p + 9.83}$	**0.97**	**0.95**	**±3**	**32**
	$\mathbf{T_w = 8.21 \times t_a - 0.41 \times q + \ + 0.53 \times d\% + 8.72}$	**0.96**	**0.96**	**±4**	**32**
HG	$T_w = 14.27 \times t_a - 0.22 \times q + 6.39$	0.83	0.78	±16	26
	$T_w = 12.01 \times t_a + 1.73 \times p + 6.82$	0.90	0.87	±11	26
	$T_w = 13.42 \times t_a + 1.50 \times d\% + 6.71$	0.88	0.86	±12	26
	$T_w = 12.94 \times t_a - 1.66 \times f\% + 9.04$	0.91	0.89	±10	26
	$\mathbf{T_w = 11.97 \times t_a - 0.86 \times q - 2.88 \times f\% + 10.28}$	**0.96**	**0.95**	**±5**	**26**
	$\mathbf{T_w = 10.78 \times t_a - 0.74 \times q + 2.62 \times p + 9.97}$	**0.94**	**0.94**	**±6**	**26**
	$\mathbf{T_w = 11.19 \times t_a - 0.77 \times q + 2.53 \times d\% + 9.18}$	**0.97**	**0.96**	**±2**	**26**
BZA	$T_w = 13.01 \times t_a - 0.15 \times q + 7.19$	0.87	0.83	±11	33
	$T_w = 11.38 \times t_a + 1.10 \times p + 7.81$	0.91	0.88	±10	33
	$T_w = 11.27 \times t_a + 0.89 \times d\% + 8.32$	0.86	0.84	±12	33
	$T_w = 11.60 \times t_a - 1.01 \times f\% + 8.49$	0.90	0.89	±9	33
	$\mathbf{T_w = 9.53 \times t_a - 0.74 \times q - 1.40 \times f\% + 9.79}$	**0.95**	**0.94**	**±5**	**33**
	$\mathbf{T_w = 9.14 \times t_a - 0.66 \times q + 1.23 \times p + 8.68}$	**0.95**	**0.95**	**±3**	**33**
	$\mathbf{T_w = 9.32 \times t_a - 0.62 \times q + 1.01 \times d\% + 8.88}$	**0.96**	**0.96**	**±4**	**33**
All rivers	$T_w = 17.49 \times t_a + 2.98$	0.49	0.44	±37	91
	$T_w = 19.34 \times t_a - 1.04 \times q + 0.99$	0.61	0.55	±33	91
	$T_w = 12.81 \times t_a + 1.55 \times p + 6.75$	0.61	0.57	±31	91
	$T_w = 16.51 \times t_a + 0.57 \times d\% + 3.77$	0.57	0.52	±34	91
	$T_w = 10.78 \times t_a - 5.21 \times f\% + 13.76$	0.66	0.62	±27	91
	$\mathbf{T_w = 13.24 \times t_a - 1.49 \times q - 2.90 \times f\% + 7.43}$	**0.91**	**0.89**	**±7**	**91**
	$\mathbf{T_w = 12.79 \times t_a - 1.73 \times q + 2.13 \times p + 5.93}$	**0.90**	**0.90**	**±8**	**91**
	$\mathbf{T_w = 12.65 \times t_a - 1.64 \times q + 2.34 \times d\% + 6.15}$	**0.88**	**0.87**	**±10**	**91**

t_a, q, $f\%$, $d\%$, and p denotes the standardized annual mean air temperature, water discharge, forest area percentage, developed land area percentage, and population density, respectively.
All bold R^2 values denote $p < 0.01$.

Fig. 6. The standardized multiple regression model estimated contribution of air temperature, water discharge, and human activities to temporal or spatio-temporal variation of water temperature in 1980–2012 (a) and predicted water temperature for 2050 under four scenarios compared to the 2000–2012 baseline condition (b) in three river segments of the Yongan River watershed. Error bars denote the standard deviations of the three models (Table 3) estimated contributions for each river segment or all three river segments. Vertical lines denote the 95% confidence interval of predicted water temperature.

reported for rivers in the U.S.A. (0.009–0.077 °C yr^{-1}, Kaushal et al., 2010; Isaak et al., 2012; Null et al., 2013a,b; Rice and Jastram, 2015), Europe (0.006–0.18 °C yr^{-1}, Moatar and Gailhard, 2006; Albek and Albek, 2009; Pekárová et al., 2011; Žganec, 2012; Jurgelėnaitė et al., 2012; Markovic et al., 2013; Lepori et al., 2014; Orr et al., 2015), and Australia (0.014–0.017 °C yr^{-1}, Webb and Nobilis, 2007). Although no relevant reports are currently available for rivers in China, the rapid economic development and urbanization in China, especially in eastern China over the past several decades, are expected to enhance rising river water temperature rates in conjunction with the interactive effects of climate change for many rivers.

Consistent with many previous studies (Markovic et al., 2013; Daraio and Bales, 2014; Rice and Jastram, 2015), this study indicated that climate warming (Fig. 2) is the major driver (81–95%) of rising river water temperature over the past 33 years (Fig. 6a). However, monthly water temperature variations tend to lag behind fluctuations in air temperature by ∼3 months (Fig. 5), which has been widely observed in previous studies with lag times ranging from several days to several months (Caissie, 2006; van Vliet et al., 2011; Gu et al., 2014; Johnson et al., 2014). The longest lag time was for the largest river segment (BZA) (Fig. 5), which implies that the larger catchment area has a longer residence time for runoff and delivery through the drainage network, resulting in

greater time required for influencing downstream river water temperature (van Vliet et al., 2011; Johnson et al., 2014). Furthermore, lag times are positively correlated with the contribution of groundwater (Gu et al., 2014; Garner et al., 2014).

Local human activities such as increasing developed land, increasing population density and decreasing forest area contributed substantially (5–19%) to the higher river temperature (Fig. 6a). Due to the influence of human activities, HG showed the most rapid river warming rate among the three river segments (Fig. 2). Higher percentage of developed area implies more impervious surfaces and yields more heated urban runoff to rivers (Kaushal et al., 2010; Lepori et al., 2014; Gu et al., 2014; Garner et al., 2014). The rapid runoff from impervious surfaces is also believed to partially contribute to a shorter lag time between changes in monthly air and river water temperature for the HG river segment (Fig. 5), which is consistent with the higher runoff coefficient in HG (Table 1). The 12% decrease in forest area and 60% increase in developed land area in catchment HG over the past 33 years (Table 1) implies a considerable loss in river riparian canopy cover and shading, which further contributes to increasing water temperature (Gu et al., 2014; DeWeber and Wagner, 2014; Simmons et al., 2014).

Due to less direct coupling to atmospheric energy exchange (both short- and long-wave radiation) as a result of the forest canopy (Luce et al., 2014), river segment HX showed the lowest river water warming rate, as well as the lowest CV of annual mean water temperature (Fig. 2). The higher population densities further imply generation of a considerable quantity of domestic and industry sewage discharge to river segment HG, which is another heat source contributing to warming of river water in urban areas (Kinouchi, 2007; Nelson and Palmer, 2007; Kaushal et al., 2010; Xin and Kinouchi, 2013; Lepori et al., 2014). This premise is supported by the higher water warming rate in the HG segment than for air temperature during the winter (Fig. 4).

Water discharge is another important driver in regulating air–water temperature dynamics and it accounted for 5–6% and ~10% of the temporal and spatio-temporal variations of annual mean river water temperature (Fig. 6a), respectively. This result is consistent with estimates for the Danube River and Elbe River where water discharge accounted for 6–11% of the temporal variation in water temperature, compared to 83–84% and 6–10% contributions from air temperature and the North Atlantic Oscillation, respectively (Markovic et al., 2013). The negative correlation observed between river water temperature and discharge in each river segment (Table 2) primarily results from reduced thermal buffering capacity and increased travel time at low discharge (Gu and Li, 2002; Webb et al., 2003; van Vliet et al., 2011). This mechanism also supports the higher warming rates observed during the dry winter season compared to the other seasons in each river segment (Fig. 5).

In terms of spatial dynamics, river segment HG having the lowest water discharge displayed the greatest response rate (Table 3) to changes in air temperature and human activities. Due to the influence of water discharge, river segment HG had significantly higher annual mean water temperature than BZA; however, no significant difference was observed between them in seasonal mean water temperature during the high flow summer and fall periods (Fig. 3). These results imply that smaller rivers and dry seasons are more sensitive to climate warming and human activities compared to larger rivers and wet seasons.

Changes in the contribution of groundwater may also have a considerable influence on water temperature (Gu et al., 2014; Garner et al., 2014). It appears that the Yongan watershed had no significant change in groundwater contributions during the study period since there were no significant changes in the runoff coefficient ($p > 0.05$, Table 1) or water discharge (Fig. 2). This implies a limited influence from changes in runoff/groundwater contributions on rising water temperatures in this study.

This study adopted a standardized multiple regression model to incorporate air temperature, local human activities and water discharge for predicting annual mean river water temperature. The strong agreement ($R^2 = 0.88$–0.97; Nash–Sutcliffe coefficient = 0.87–0.96, Table 3) between modeled and observed river water temperatures validates the reliability and robustness of these model results (Chen et al., 2014). The model is simple and easily applied to predict river water temperature across various sites and time periods from commonly available data. Another important feature of these models is the ability to quantify the contribution of individual drivers to variations in annual mean river water temperature. Consistent results determined by the various models that incorporate different independent variables for expressing local human activities at both temporal and spatio-temporal scales (Fig. 6a) further indicate the robustness of the methodology. Due to differences in watershed characteristics, the drivers and function types may change and require optimization for application to different watersheds. However, the methodology proposed in this study should be widely applicable to other watersheds.

Finally, we evaluated four scenarios for future developments affecting river water temperature by 2050 (Fig. 6b). The range of model predicted results roughly represents the upper and lower bounds for future water temperatures in response to local anthropogenic activities and climate change, providing a baseline for adopting relevant water management strategies. If we assume that an increase of 1 °C in river water temperature would result in a 0.2 mg L^{-1} decrease in the equilibrium DO concentration (El-Jabi et al., 2014) and a ~18% increase in annual mean phytoplankton Chl-a concentration (Ye et al., 2011), the four projected scenarios predict a 0.06–0.35 mg L^{-1} decrease in equilibrium DO concentration and a 6–33% increase in algal biomass flux to downstream waters by 2050 merely because of rising water temperature. Given the excessive nutrient and oxygen-demanding substances present in the rivers and coastal waters in Eastern China due to intensive human activities (Li et al., 2007; Gao and Zhang, 2010), such changes in heat, algal biomass and DO fluxes in rivers will have a considerable potential to aggravate eutrophication (including harmful algal blooms) and persistent hypoxia of the downstream coastal waters in the future.

Rising river water temperatures also pose a serious risk for endangered cold-water species living near their thermal maximum (Null et al., 2013a,b). Considering the warming of air temperature predicted for the next several decades by the IPCC (2013) and local government (Huang et al., 2014), rising river water temperature in the future is unavoidable, since river water temperature is largely governed by air temperature in the Yongan watershed, as well as in many watersheds worldwide (Markovic et al., 2013; Daraio and Bales, 2014). Therefore, the adverse effects of increasing water temperature should be further considered in river and coastal water management (Moatar and Gailhard, 2006; Caissie, 2006). Although local efforts will have a limited impact on climate warming, increasing water temperature could be somewhat mitigated through constructing riparian buffers for avoiding direct heated urban runoff from entering rivers, increasing vegetation cover and river shading (Markovic et al., 2013; Lepori et al., 2014), and cooling domestic and industrial sewage prior to discharge into rivers. Furthermore, appropriate dam regulation may be able to cool water and offer a potential mitigation strategy for climate change-induced river warming (Null et al., 2013a; Rice and Jastram, 2015).

5. Conclusion

This study presents the first historically explicit analysis of river water temperature trends for a typical watershed in eastern China that is subject to significant climate change and rapid human

development. In three river segments of the Yongan watershed, water temperature increased by 0.029–0.046 °C yr^{-1} due to climate warming ($\sim$0.050 °C yr^{-1}) and increasing human activities over the 1980–2012 period. Heterogeneity of warming rates existed across seasons and river segments, with the lower flow river segment and dry winter season demonstrating a more pronounced response to climate warming and human activities. A standardized multiple regression model that incorporates air temperature, local human activities and water discharge provided a simple and efficient method for predicting annual mean river water temperature and identifying the contribution from the individual principal drivers. For the Yongan watershed, climate warming and increasing local human activities were estimated to contribute 81–95% and 5–19% of the observed rising river water temperature, respectively. Models forecast a 0.32–1.76 °C increase in river temperatures by 2050 compared to 2000–2012 baseline conditions based on four future scenarios. Such predicted warming magnitudes have a considerable potential to aggravate river water quality degradation and coastal water eutrophication in the future. The negative effect of increasing water temperature due to changes in climate, local human activities and hydrology should be considered in developing watershed environmental and ecological management strategies, as well as adaptation plans for climate change.

Acknowledgements

References

Albek, M., Albek, E., 2009. Stream temperature trends in Turkey. Clean 37, 142–149.

Arismendi, I., Johnson, S.L., Dunham, J.B., Haggerty, R., Hockman-Wert, D., 2012. The paradox of cooling streams in a warming world: regional climate trends do not parallel variable local trends in stream temperature in the Pacific continental United States. Geophys. Res. Lett. 39, L10401.

Caissie, D., 2006. The thermal regime of rivers: a review. Freshwater Biol. 51, 1389–1406.

Chen, D.J., Huang, H., Hu, M.P., Dahlgren, R.A., 2014. Influence of lag effect, soil release, and climate change on watershed anthropogenic nitrogen inputs and riverine export dynamics. Environ. Sci. Technol. 48, 5683–5690.

Daraio, J.A., Bales, J.D., 2014. Effects of land use and climate change on stream temperature I: daily flow and stream temperature projections. J. Am. Water Resour. Assoc. 50, 1155–1176.

DeWeber, J.T., Wagner, T., 2014. A regional neural network ensemble for predicting mean daily river water temperature. J. Hydrol. 517, 187–200.

El-Jabi, N., Caissie, D., Turkkan, N., 2014. Water quality index assessment under climate change. J. Water Resour. Prot. 6, 533–542.

Gao, C., Zhang, T.L., 2010. Eutrophication in a Chinese context: understanding various physical and socio-economic aspects. Ambio 39, 385–393.

Garner, G., Hannah, D.M., Sadler, J.P., Orr, H.G., 2014. River temperature regimes of England and Wales: spatial patterns, inter-annual variability and climatic sensitivity. Hydrol. Process. 28, 5583–5598.

Gu, C.H., Anderson Jr., W.P., Colby, J.D., Coffey, C.L., 2014. Air-stream temperature correlation in forested and urban headwater streams in the Southern Appalachians. Hydrol. Process. http://dx.doi.org/10.1002/hyp.10225.

Gu, R.R., Li, Y., 2002. River temperature sensitivity to hydraulic and meteorological parameters. J. Environ. Manage. 66, 43–56.

Huang, H., Chen, D.J., Zhang, B.F., Zeng, L.Z., Dahlgren, R.A., 2014. Modeling and forecasting riverine dissolved inorganic nitrogen export using anthropogenic nitrogen inputs, hydroclimate, and land-use change. J. Hydrol. 517, 95–104.

IPCC (Intergovernmental Panel on Climate Change), 2013. Climate change 2013: the physical science basis, summary for policymakers. Working Group 1 Contribution to the Fifth Assessment Report. <http://www.climatechange2013.org/images/uploads/WGIAR5- SPM_Approved27Sep2013.pdf>.

Isaak, D.J., Wollrab, S., Horan, D., Chandler, G., 2012. Climate change effects on stream and river temperatures across the northwest U.S. from 1980–2009 and implications for salmonid fishes. Climatic Change 113, 499–524.

Johnson, M.F., Wilby, R.L., Toone, J.A., 2014. Inferring air–water temperature relationships from river and catchment properties. Hydrol. Process. 28, 2912–2928.

Jurgelėnaitė, A., Kriaučiūnienė, J., Šarauskienė, D., 2012. Spatial and temporal variation in the water temperature of Lithuanian rivers. Baltica 25, 65–76.

Kaushal, S.S., Likens, G.E., Jaworski, N.A., Pace, M.L., Sides, A.M., Seekell, D., Belt, K.T., Secor, D.H., Wingate, R., 2010. Rising stream and river temperatures in the United States. Frontiers Ecol. Environ. 8, 461–466.

Kinouchi, T., 2007. Impact of long-term water and energy consumption in Tokyo on wastewater effluent: implications for the thermal degradation of urban streams. Hydrol. Process. 21, 1207–1216.

Langan, S.J., Johnston, U.L., Donaghy, M.J., Youngson, A.F., Hay, D.W., Soulsby, C., 2001. Variation in river water temperatures in an upland stream over a 30-year period. Sci. Total Environ. 265, 195–207.

Lepori, F., Pozzoni, M., Pera, S., 2014. What drives warming trends in streams? a case study from the Alpine Foothills. River Res. Appl. http://dx.doi.org/10.1002/rra.2763.

Li, M.T., Xu, K.Q., Watanabe, M., Chen, Z.Y., 2007. Long-term variations in dissolved silicate, nitrogen, and phosphorus flux from the Yangtze River into the East China Sea and impacts on estuarine ecosystem. Estuar. Coast Shelf. Sci. 71, 3–12.

Liu, B., Yang, D., Ye, B., Berezovskaya, S., 2005. Long-term open-water season stream temperature variations and changes over Lena River Basin in Siberia. Global Planet. Change 48, 96–111.

Luce, C., Staab, B., Kramer, M., Wenger, S., Isaak, D., McConnell, C., 2014. Sensitivity of summer stream temperatures to climate variability in the Pacific Northwest. Water Resour. Res. 50, 3428–3443.

Markovic, D., Scharfenberger, U., Schmutz, S., Pletterbauer, F., Wolter, C., 2013. Variability and alterations of water temperatures across the Elbe and Danube River Basins. Climatic Change 119, 375–389.

Moatar, F., Gailhard, J., 2006. Water temperature behaviour in the River Loire since 1976 and 1881. C. R. Geosci. 338, 319–328.

Mohseni, O., Stefan, H.G., 1999. Stream temperature/air temperature relationship: a physical interpretation. J. Hydrol. 218, 128–141.

Moore, R.D., Spittlehouse, D.L., Story, A., 2005. Riparian microclimate and stream temperature response to forest harvesting: a review. J. Am. Water Resour. Assoc. 41, 813–834.

Nelson, K.C., Palmer, M.A., 2007. Stream temperature surges under urbanization and climate change: data, models, and responses. J. Am. Water Resour. Assoc. 43, 440–452.

Null, S.E., Ligare, S.T., Viers, J.H., 2013a. A method to consider whether dams mitigate climate change effects on stream temperatures. J. Am. Water Resour. Assoc. 49, 1456–1472.

Null, S.E., Viers, J.H., Deas, M.L., Tanaka, S.K., Mount, J.F., 2013b. Stream temperature sensitivity to climate warming in California's Sierra Nevada: impacts to coldwater habitat. Climatic Change 116, 149–170.

Orr, H.G., Simpson, G.L., des Clers, S., Watts, G., Hughes, M., Hannaford, J., Dunbar, M.J., Laizé, C.L.R., Wilby, R.L., Battarbee, R.W., Evans, R., 2015. Detecting changing river temperatures in England and Wales. Hydrol. Process. 29, 752–766.

Ozaki, N., Fukushima, T., Kojiri, T., 2008. Simulation of the effects of the alteration of the river basin land use on river water temperature using the multi-layer mesh-typed runoff model. Ecol. Model. 215, 159–169.

Pekárová, P., Miklánek, P., Halmová, D., Onderka, M., Pekár, J., Kučárová, K., Liová, S., Škoda, P., 2011. Long-term trend and multi-annual variability of water temperature in the pristine Bela River basin (Slovakia). J. Hydrol. 400, 333–340.

Rice, K.C., Jastram, J.D., 2015. Rising air and stream-water temperatures in Chesapeake Bay region, USA. Climatic Change 128, 127–138.

Seekell, D.A., Pace, M.L., 2011. Climate change drives warming in the Hudson River Estuary, New York (USA). J. Environ. Monit. 13, 2321–2327.

Simmons, J.A., Anderson, M., Dress, W., Hanna, C., Hornbach, D.J., Janmaat, A., Kuserk, F., March, J.G., Murray, T., Niedzwiecki, J., Panvini, D., Pohlad, B., Thomas, C., Vasseur, L., 2014. A comparison of the temperature regime of short stream segments under forested and non-forested riparian zones at eleven sites across North America. River Res. Appl. http://dx.doi.org/10.1002/rra.2796.

van Vliet, M.T.H., Ludwig, F., Zwolsman, J.J.G., Weedon, G.P., Kabat, P., 2011. Global river temperatures and sensitivity to atmospheric warming and changes in river flow. Water Resour. Res. 47, W02544.

van Vliet, M.T.H., Yearsley, J.R., Franssen, W.H.P., Ludwig, F., Haddeland, I., Lettenmaier, D.P., Kabat, P., 2012. Coupled daily streamflow and water temperature modelling in large river basins. Hydrol. Earth Syst. Sci. 16, 4303–4321.

Webb, B.W., Clack, P.D., Walling, D.E., 2003. Water–air temperature relationships in a Devon river system and the role of flow. Hydrol. Process. 17, 3069–3084.

Webb, B.W., Hannah, D.M., Moore, R.D., Brown, L.E., Nobilis, F., 2008. Recent advances in stream and river temperature research. Hydrol. Process. 22, 902–918.

Webb, B.W., Nobilis, F., 2007. Long-term changes in river temperature and the influence of climatic and hydrological factors. Hydrol. Sci. J. 52, 74–85.

Xin, Z.H., Kinouchi, T., 2013. Analysis of stream temperature and heat budget in an urban river under strong anthropogenic influences. J. Hydrol. 489, 16–25.

Ye, C., Shen, Z.M., Zhang, T., Fan, M.H., Lei, Y.M., Zhang, J.D., 2011. Long-term joint effect of nutrients and temperature increase on algal growth in Lake Taihu, China. J. Environ. Sci. 23, 222–227.

Žganec, K., 2012. The effects of water diversion and climate change on hydrological alteration and temperature regime of karst rivers in central Croatia. Environ. Monit. Assess. 184, 5705–5723.